Some knowledge of ion trap for QIP

C.M.L[1]

[1] *Center for Quantum Information, Institute of Interdisciplinary Information Science, Tsinghua University**

I. RADIO-FREQUENCY TRAPS FOR SINGLE ION

Ions are trapped in a dynamic electric field (rf or Pual trap):

$$\Phi(x,y,z,t)=\frac{U}{2}(\alpha x^2+\beta y^2+\gamma z^2)+\frac{\tilde{U}}{2}\cos(\omega_{rf}t)(\alpha' x^2+\beta' y^2+\gamma' z^2) \tag{1}$$

For more details, please refer to the review article [1].

In general, the ideal potential near the center of the Paul trap (linear trap) is of the form:

$$\Phi(x,y,z,t)=\frac{U}{2}(-\gamma/2(x^2+y^2)+\gamma z^2)+\frac{\tilde{U}}{2}\cos(\omega_{rf}t)\alpha'(x^2-y^2) \tag{2}$$

i.e. the x-y plane is dynamical confinement and the z-axis is static potential confinement.

II. LASER-ION INTERACTION[2]

A. general theory

The Halmitonian of the trapped ion illuminated by the laser is: $\hat{H}=\hat{H}_0+\hat{V}$, where the $\hat{H}_0$ is $\hbar\omega_0\hat{\sigma}_+\hat{\sigma}_-+\hbar\nu\hat{a}^\dagger\hat{a}$. We now derive the laser-ion interaction $\hat{V}$, We only consider the electric field of laser,

$$\mathbf{E}=\frac{\mathbf{E}_0}{2}\left(e^{i(\omega_L t-\mathbf{k}\cdot\mathbf{R}+\varphi_L)}+e^{-i(\omega_L t-\mathbf{k}\cdot\mathbf{R}+\varphi_L)}\right) \tag{3}$$

where $\mathbf{R}$ is the position vector of ions and φ_L is phase factor of laser field. We only consider dipole interation (where $\mathbf{d}=e\mathbf{r}$),

$$\hat{V}=\hat{V}^{DP}+\hat{V}^{I-B}=-\mathbf{d}\cdot\mathbf{E}(t,\mathbf{R})-\frac{1}{2m}(\hat{\mathbf{P}}\cdot(\mathbf{B}\times\mathbf{d})+(\mathbf{B}\times\mathbf{d})\cdot\hat{\mathbf{P}}) \tag{4}$$

The position of the ion along the z axis is

$$\hat{z}=\bar{z}+\kappa z_0(\hat{a}^\dagger+\hat{a}) \tag{5}$$

* caiml16@mails.tsinghua.edu.cn

Then the dipole interaction Hamiltonian is

$$\hat{V} = -e(\mathbf{r}_{eg}\hat{\sigma}_+ + \mathbf{r}_{eg}\hat{\sigma}_-) \cdot \frac{\mathbf{E}_0}{2}(e^{i(\omega_L t - \eta(\hat{a}^\dagger + \hat{a}) + \phi)} + H.c.) \tag{6}$$

Where $\mathbf{r}_{eg} = \langle e|\,\hat{\mathbf{r}}\,|g\rangle$, $\eta = \kappa z_0 k \cos\theta$ is the Lamb-Dicke parameter indicating the ratio between ion-motional extent and light wavelength, and $\phi = \varphi_L - k\cos\theta\bar{z}$. We transfer into the interaction picture by sandwiching the $\hat{V}$ by $\hat{U}_0^\dagger$ and $\hat{U}_0$, where $\hat{U}_0 = \exp\Big(-i\hat{H}_0 t\Big)$. (We will set $\hbar$ as 1)

$$\hat{V}_{int} = \hat{U}_0^\dagger \hat{V} \hat{U}_0 = -e(\mathbf{r}_{eg}\hat{\sigma}_+ e^{i\omega_0 t} + \mathbf{r}_{eg}\hat{\sigma}_- e^{-i\omega_0 t}) \cdot \frac{\mathbf{E}_0}{2}(\exp\Big(i(\omega_L t - \eta(\hat{a}^\dagger e^{i\nu t} + \hat{a}e^{-i\nu t}) + \phi)\Big) + H.c.) \tag{7}$$

By rotation wave approximation, we get:

$$\hat{V} = -e\mathbf{r}_{eg} \cdot \frac{\mathbf{E}_0}{2}\hat{\sigma}_+ e^{-i(\delta t + \phi)} \exp\Big(i\eta(\hat{a}^\dagger e^{i\nu t} + \hat{a}e^{-i\nu t})\Big) + H.c. \tag{8}$$

where $\delta = \omega_L - \omega_0$ is the detuning. We set $\lambda = -e\mathbf{r}_{eg} \cdot \mathbf{E}_0 e^{-i\phi}$, then the $\hat{V}$ is

$$\hat{V} = \frac{\lambda}{2}\hat{\sigma}_+ e^{-i\delta t} \exp\Big(i\eta(\hat{a}^\dagger e^{i\nu t} + \hat{a}e^{-i\nu t})\Big) + H.c. \tag{9}$$

Next, let us assume the detuning δ of the laser frequency ω_L from the atomic frequency ω_0 for the vibrational frequency ν in the form:

$$\delta = \omega_L - \omega_0 = k\nu,\ k = 0, \pm 1, \pm 2, \ldots \tag{10}$$

We apply BCH theorem to equation (9):

$$\hat{V} = \frac{\lambda}{2}\hat{\sigma}_+ e^{-\eta^2/2} \sum_{n,m=0}^{\infty} (i\eta)^{n+m} \frac{(a^\dagger)^n}{n!}\frac{a^m}{m!} e^{i\nu t(n-m-k)} + H.c. \tag{11}$$

If the laser is tuned at the frequency ω_L such that $k > 0$, the spectral line is termed the kth blue sideband. For $k = 0$ the line is called the carrier and for $k < 0$ we refer to the kth red sideband because the laser is red (blue) detuned from the atomic frequency ω_0

We neglect the off-resonance terms in (11), i.e. we neglect all the $n - m - k \neq 0$ and rewrite the (11) for $k \geq 0$ in the form:

for $k \geq 0$

$$\hat{V}^+ = \frac{\lambda}{2}\hat{\sigma}_+ e^{-\eta^2/2}(i\eta)^k (a^\dagger)^k F(a^\dagger, a) + H.c. \tag{12}$$

for $k < 0$

$$\hat{V}^- = \frac{\lambda}{2}\hat{\sigma}_+ e^{-\eta^2/2}(i\eta)^{|k|} F(a^\dagger, a) a^{|k|} + H.c. \tag{13}$$

Where$F(a^\dagger, a) = \sum_{n=0}^{\infty} \frac{(a^\dagger)^n}{(n+|k|)!} \frac{a^n}{n!}(-\eta^2)^n$

Becuase $a^n |m\rangle = \sqrt{\frac{m!}{(m-n)!}} |m-n\rangle$ and $(a^\dagger)^n |m\rangle = \sqrt{\frac{(m+n)!}{m!}} |m+n\rangle$

$$\sum_{m=0}^{\infty} (a^\dagger)^{k+n} a^n |m\rangle \langle m| = \sum_{m=0}^{\infty} \sqrt{\frac{m!(m+k)!}{((m-n)!)^2}} |m+k\rangle \langle m| \tag{14}$$

Then, $F(a^\dagger, a)$ becomes

$$\begin{aligned} F(a^\dagger, a) &= \sum_{n=0}^{\infty} \frac{(a^\dagger)^n}{(n+|k|)!} \frac{a^n}{n!}(-\eta^2)^n = \sum_{n=0}^{\infty}\sum_{m=0}^{\infty} (-\eta^2)^n \frac{(a^\dagger)^n}{(n+|k|)!} \frac{a^n}{n!} |m\rangle \langle m| \\ &= \sum_{n=0}^{\infty}\sum_{m=n}^{\infty} (-\eta^2)^n \frac{\sqrt{m!(m+k)!}}{n!(n+k)!(m-n)!} |m+k\rangle \langle m| \\ &= \sum_{m=0}^{\infty} \left(\sum_{n=0}^{m} (-\eta)^2 \frac{(m+k)!}{n!(n+k)!(m-n)!} \right) \sqrt{\frac{m!}{(m+k)!}} |m+k\rangle \langle m| \\ &= \sum_{m=0}^{\infty} L_m^k(\eta^2) \sqrt{\frac{m!}{(m+k)!}} |m+k\rangle \langle m| \end{aligned} \tag{15}$$

Where $L_m^k(x) = \sum_{n=0}^{m} \frac{(-x)^n}{n!} \binom{m+k}{m-n}$ is the generalized Laguerre polynomial. So the $\hat{V}^+$ can be write as:

$$\hat{V}_k^+ = \sum_{m=0}^{\infty} \left(\frac{\Omega^{m,k}}{2} |e\rangle \langle g| \otimes |m+k\rangle \langle m| + H.c. \right) \tag{16}$$

It's the same that when $k < 0$, $\hat{V}^-$ is

$$\hat{V}_k^- = \sum_{m=0}^{\infty} \left(\frac{\Omega^{m,|k|}}{2} |e\rangle \langle g| \otimes |m\rangle \langle m+|k|| + H.c. \right) \tag{17}$$

Where $\Omega^{m,|k|} = \lambda e^{-\eta^2/2} (i\eta)^{|k|} L_m^{|k|}(\eta^2) \sqrt{\frac{m!}{(m+|k|)!}}$, so $\Omega^{m,|k|} = \left|\Omega^{m,|k|}\right| e^{i\frac{|k|\pi}{2} - i\phi}$

The time-independent Hamiltonian is $\hat{U}^\pm = \exp\left(-i\hat{V}^\pm t\right)$ We can expand it and caculate $(\hat{V}^+)^2$, $(\hat{V}^+)^3$ to find out the rule.

For $k \geq 0$:

$$\begin{aligned} \hat{U}_k^+ = &\sum_{m=0}^{\infty} \cos\left(\frac{\left|\Omega^{m,k}\right| t}{2} \right) (|g\rangle \langle g| \otimes |m\rangle \langle m| + |e\rangle \langle e| \otimes |m+k\rangle \langle m+k|) \\ &- i \sum_{m=0}^{\infty} \sin\left(\frac{\left|\Omega^{m,k}\right| t}{2} \right) (|e\rangle \langle g| \otimes |m+k\rangle \langle m| \, e^{i(\frac{k\pi}{2} - \phi)} + H.c.) + \sum_{m=0}^{k-1} |e\rangle \langle e| \otimes |m\rangle \langle m| \end{aligned} \tag{18}$$

For $k < 0$:

$$\begin{aligned} \hat{U}_k^- = &\sum_{m=0}^{\infty} \cos\left(\frac{\left|\Omega^{m,|k|}\right| t}{2} \right) (|g\rangle \langle g| \otimes |m+|k|\rangle \langle m+|k|| + |e\rangle \langle e| \otimes |m\rangle \langle m|) \\ &- i \sum_{m=0}^{\infty} \sin\left(\frac{\left|\Omega^{m,|k|}\right| t}{2} \right) (|e\rangle \langle g| \otimes |m\rangle \langle m+|k|| \, e^{i(\frac{|k|\pi}{2} - \phi)} + H.c.) + \sum_{m=0}^{|k|-1} |g\rangle \langle g| \otimes |m\rangle \langle m| \end{aligned} \tag{19}$$

In what follows we shall assume that all motional modes are in the Lamb-Dicke regime characterized by the Lamb-Dicke limit. Then $\Omega^{m,|k|} \approx \lambda(i\eta)^{|k|}(\frac{(m+|k|)!}{m!})^{\frac{1}{2}}\frac{1}{|k|!}$

For the purpose of coherent manipulations with internal states of cold trapped ions we shall be primarily interested in the interaction on the carrier ($k = 0$) and on the first red sideband ($k = -1$) which shall be used for the construction of a wide class of quantum logic gates.

For $k = 0$

$$\hat{A} = \sum_{m=0}^{\infty} \cos\left(\frac{|A_m|t}{2}\right)(|g\rangle\langle g| \otimes |m\rangle\langle m| + |e\rangle\langle e| \otimes |m\rangle\langle m|)$$
$$- i\sum_{m=0}^{\infty} \sin\left(\frac{|A_m|t}{2}\right)(|e\rangle\langle g| \otimes |m\rangle\langle m| e^{-i\phi} + H.c.) \tag{20}$$

For $k = -1$

$$\hat{B} = \sum_{m=0}^{\infty} \cos\left(\frac{|B_m|t}{2}\right)(|g\rangle\langle g| \otimes |m+1\rangle\langle m+1| + |e\rangle\langle e| \otimes |m\rangle\langle m|)$$
$$- i\sum_{m=0}^{\infty} \sin\left(\frac{|B_m|t}{2}\right)(|e\rangle\langle g| \otimes |m\rangle\langle m+1| e^{-i(\phi-\frac{\pi}{2})} + H.c.) + |g\rangle\langle g| \otimes |0\rangle\langle 0| \tag{21}$$

Where $A_m = \lambda$ and $B_m = \lambda\eta(m+1)^{1/2}$

B. Raman interaction

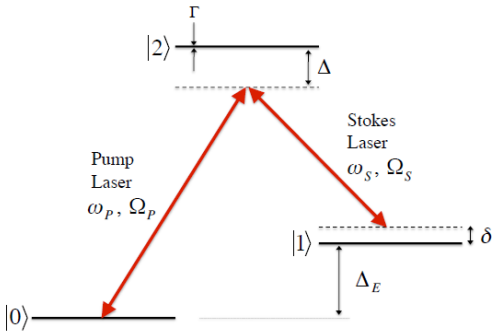

FIG. 1. level scheme of Raman interaction

We now consider the Raman laser beams interacting with single ion. As we can see from figure1, there are two laser beams coupling ground state ($|0\rangle$) and excited state ($|1\rangle$), excited state and a auxiliary state ($|2\rangle$), respectively. The Hamiltonian under intraction picture is (8)

$$V_{Raman} = (\frac{\hbar\Omega_P^{21}}{2}\hat{\sigma}_{21}e^{-i(\Delta+\Delta_E)t} + \frac{\hbar\Omega_P^{20}}{2}\hat{\sigma}_{20}e^{-i\Delta t})\exp\left(i\eta_P(a^\dagger e^{i\nu t} + ae^{-i\nu t})\right)$$
$$+ (\frac{\hbar\Omega_S^{21}}{2}\hat{\sigma}_{21}e^{-i(\Delta-\delta)t} + \frac{\hbar\Omega_S^{20}}{2}\hat{\sigma}_{20}e^{-i(\Delta-\delta-\Delta_E)t})\exp\left(i\eta_S(a^\dagger e^{i\nu t} + ae^{-i\nu t})\right) + H.c. \tag{22}$$

where $\Omega_x^{i,j} = -\frac{e\mathbf{r}_{i,j}\cdot\mathbf{E}_x}{\hbar}e^{-i\phi_x}$ $(i,j=0,1,2$ and $x=P,S)$ and $\hat{\sigma}_{i,j} = |i\rangle\langle j|$. expanding the motional degree of freedom term and only reserve the leading term we get

$$\begin{aligned} V_{Raman} = & \frac{\hbar\Omega_P^{21}}{2}\hat{\sigma}_{21}e^{-i(\Delta+\Delta_E)t} + \frac{\hbar\Omega_P^{20}}{2}\hat{\sigma}_{20}e^{-i\Delta t} \\ & + \frac{\hbar\Omega_S^{21}}{2}\hat{\sigma}_{21}e^{-i(\Delta-\delta)t} + \frac{\hbar\Omega_S^{20}}{2}\hat{\sigma}_{20}e^{-i(\Delta-\delta-\Delta_E)t} + H.c. \end{aligned} \tag{23}$$

transforming to a new reference by $\hat{U} = e^{i\delta t|1\rangle\langle 1|+i\Delta t|2\rangle\langle 2|}$, we get the Hamiltonian under this reference

$$\begin{aligned} \tilde{H} = & -\hbar\delta|1\rangle\langle 1| - \hbar\Delta|2\rangle\langle 2| + (\frac{\hbar\Omega_P^{20}}{2}|2\rangle\langle 0| + \frac{\hbar\Omega_S^{21}}{2}|2\rangle\langle 1| \\ & + \frac{\hbar\Omega_S^{20}}{2}|2\rangle\langle 0|e^{i(\Delta_E+\delta)t} + \frac{\hbar\Omega_P^{21}}{2}|2\rangle\langle 1|e^{-i(\Delta_E+\delta)t} + H.c.) \end{aligned} \tag{24}$$

Firstly, we won't consider the cross coupling term, then the Hamiltonian is time-independent

$$\begin{aligned} \tilde{H} = & -\hbar\delta|1\rangle\langle 1| - \hbar\Delta|2\rangle\langle 2| \\ & + \left(\frac{\hbar\Omega_P^{20}}{2}|2\rangle\langle 0| + \frac{\hbar\Omega_S^{21}}{2}|2\rangle\langle 1| + H.c.\right) \end{aligned} \tag{25}$$

if we set the internal state as $|\psi(t)\rangle = c_0(t)|0\rangle + c_1(t)|1\rangle + c_2(t)|2\rangle$, then the motion equation of c_0, c_1, c_2 is

$$\begin{aligned} i\dot{c}_0 &= \frac{(\Omega_{20}^P)^*}{2}c_2 \\ i\dot{c}_1 &= -\delta c_1 + \frac{(\Omega_{21}^S)^*}{2}c_2 \\ i\dot{c}_2 &= \frac{\Omega_{20}^P}{2}c_0 + \frac{\Omega_{21}^S}{2}c_1 - \Delta c_2 \end{aligned} \tag{26}$$

assume that Δ is much larger than Ω_{20}^P and Ω_{21}^S [3], then the population porbability of $|2\rangle$ will oscillate much faster than those of $|0\rangle$ and $|1\rangle$, so we can set $\dot{c}_2$ as zero and get $c_2 = \frac{\Omega_{20}^P c_0 + \Omega_{21}^S c_1}{2\Delta}$. We will get the effective two level system

$$\begin{aligned} i\dot{c}_0 &= \Lambda_0 c_0 + \frac{\Omega_R}{2}c_1 \\ i\dot{c}_1 &= \frac{\Omega_R^*}{2} + (\Lambda_1 - \delta)c_1 \end{aligned} \tag{27}$$

where $\Lambda_0 = \frac{|\Omega_{20}^P|^2}{4\Delta}$, $\Lambda_1 = \frac{|\Omega_{21}^S|^2}{4\Delta}$ and $\Omega_R = \frac{(\Omega_{20}^P)^*\Omega_{21}^S}{2\Delta}$ in order to solve this motion equations, we apply a unitary transformation $U = e^{i\Lambda_0 t}$ to the wave function and get

$$\begin{aligned} i\dot{\tilde{c}}_0 &= \frac{\Omega_R}{2}\tilde{c}_1 \\ i\dot{\tilde{c}}_1 &= \frac{\Omega_R^*}{2}\tilde{c}_0 + (\Lambda_1 - \Lambda_0 - \delta)\tilde{c}_1 \end{aligned} \tag{28}$$

if the initial condition is $c_0(0) = 1$ and $c_1(0) = 0$, then we get the solution for population probability of $|0\rangle$ and $|1\rangle$

$$|c_0(t)|^2 = 1 + \frac{\Omega_R^2}{2\Omega^2}(\cos(\Omega t) - 1)$$
$$|c_1(t)|^2 = \frac{\Omega_R^2}{2\Omega^2}(1 - \cos(\Omega t)) \tag{29}$$

where $\Omega = \sqrt{\Omega_R^2 + \delta_{eff}^2}$ and $\delta_{eff} = \Lambda_1 - \Lambda_0 - \delta$. Obviously we see a Rabi oscillation between the ground and excited state, for complete inversion of population, $\delta_{eff} = 0$.
Now we consider the cross coupling term,

III. QUANTUM GATES

A. single-qubit gate

A single-qubit gate is defined in the matrix form in the basis $\{|g\rangle, |e\rangle\}$ as follows:

$$\hat{R}(\theta, \phi) = \begin{pmatrix} \cos(\theta/2) & e^{i\phi}\sin(\theta/2) \\ -e^{-i\phi}\sin(\theta/2) & \cos(\theta/2) \end{pmatrix} \tag{30}$$

The single-qubit rotation can be performed on a selected ion from the ion string in the Lamb-Dicke regime by applying the unitary evolution operator $\hat{A}$ (20)
If we apply the arbitrary choice of the phase factor ($\phi \to \phi + \pi/2$). Then $\hat{A}$ becomes:

$$\hat{A}(\phi) = \sum_{m=0}^{\infty} \cos\left(\frac{l\pi}{2}\right)(|g\rangle\langle g| \otimes |m\rangle\langle m| + |e\rangle\langle e| \otimes |m\rangle\langle m|)$$
$$+ \sum_{m=0}^{\infty} \sin\left(\frac{l\pi}{2}\right)(-|e\rangle\langle g| \otimes |m\rangle\langle m| e^{-i\phi} + H.c.) \tag{31}$$

where $l\pi = |\lambda|t$. The operator is obviously equivalent to (30). and it corresponds to the ion illuminated by the laser beam on the carrier($\omega_L = \omega_0$) with the laser pulse duration $t = l\pi/|\lambda|$

B. Cirac-Zoller gate

The implementation of the two-qubit CNOT gate on two selected ions in the ion string requires the introduction of a third auxiliary internal level $|r\rangle$. Two unitary evolution operators corresponding to laser pulses driven on the first red sideband.$|g\rangle \leftrightarrow |e\rangle$ with atomic frequency $\omega_0^{eg} = (E_e - E_g)/\hbar$ and for $|e\rangle \leftrightarrow |g\rangle$ with $\omega_0^{rg} = (E_r - E_g)/\hbar$. They are given by (If we apply the

arbitrary choice of the phase factor ($\phi \to \phi + \pi/2$)):

$$\hat{B}^{l,I}(\phi) = \cos\left(\frac{l\pi}{2}\right)(|e\rangle\langle e| \otimes |0\rangle\langle 0| + |g\rangle\langle g| \otimes |1\rangle\langle 1|) - i\sin\left(\frac{l\pi}{2}\right)(|e\rangle\langle g| \otimes |0\rangle\langle 1| e^{-i\phi} + H.c.) + |g\rangle\langle g| \otimes |0\rangle\langle 0| + (m \geq 1 \quad \text{terms}) \tag{32}$$

for coupling $|g\rangle$ and $|e\rangle$, and:

$$\hat{B}^{l,II}(\phi) = \cos\left(\frac{l\pi}{2}\right)(|r\rangle\langle r| \otimes |0\rangle\langle 0| + |g\rangle\langle g| \otimes |1\rangle\langle 1|) - i\sin\left(\frac{l\pi}{2}\right)(|r\rangle\langle g| \otimes |0\rangle\langle 1| e^{-i\phi} + H.c.) + |g\rangle\langle g| \otimes |0\rangle\langle 0| + (m \geq 1 \quad \text{terms}) \tag{33}$$

for coupling $|g\rangle$ and $|r\rangle$. Where $l\pi = |\lambda|\eta t$

We do not have to condsider those terms on higher vibrational levels for $m \geq 2$ because the ions are assumed to be cooled to the ground motional state $|n = 0\rangle$

The two-qubit CNOT gate on ith and jth ions is operator sequence $\hat{A}_j^{1/2}(\pi)\hat{B}_i^{1,I}(0)\hat{B}_j^{2,II}(0)\hat{B}_i^{1,I}(0)\hat{A}_j^{1/2}(0)$

The middle sequence of $\hat{B}$ can be schematically represented as follows:

$$\begin{aligned}
&|g_i\rangle|g_j\rangle|0\rangle \xrightarrow{\hat{B}_i^{1,I}(0)} |g_i\rangle|g_j\rangle|0\rangle \xrightarrow{\hat{B}_j^{2,II}(0)} |g_i\rangle|g_j\rangle|0\rangle \xrightarrow{\hat{B}_i^{1,I}(0)} |g_i\rangle|g_j\rangle|0\rangle \\
&|g_i\rangle|e_j\rangle|0\rangle \xrightarrow{\hat{B}_i^{1,I}(0)} |g_i\rangle|e_j\rangle|0\rangle \xrightarrow{\hat{B}_j^{2,II}(0)} |g_i\rangle|e_j\rangle|0\rangle \xrightarrow{\hat{B}_i^{1,I}(0)} |g_i\rangle|g_j\rangle|0\rangle \\
&|e_i\rangle|g_j\rangle|0\rangle \xrightarrow{\hat{B}_i^{1,I}(0)} -i|g_i\rangle|g_j\rangle|1\rangle \xrightarrow{\hat{B}_j^{2,II}(0)} i|g_i\rangle|g_j\rangle|1\rangle \xrightarrow{\hat{B}_i^{1,I}(0)} |e_i\rangle|g_j\rangle|0\rangle \\
&|e_i\rangle|e_j\rangle|0\rangle \xrightarrow{\hat{B}_i^{1,I}(0)} -i|g_i\rangle|e_j\rangle|1\rangle \xrightarrow{\hat{B}_j^{2,II}(0)} -i|g_i\rangle|e_j\rangle|1\rangle \xrightarrow{\hat{B}_i^{1,I}(0)} -|e_i\rangle|e_j\rangle|0\rangle
\end{aligned} \tag{34}$$

Refering to the original article of Cirac and Zoller [4] for a simpler deduction of Cirac-Zoller gate.

C. Mølmer-Sørensen gate[5][6][7]

According to (16) and (17), the first red sideband is $\hat{V}_{-1}^-$, the first blue sideband is $\hat{V}_1^+$:

$$\begin{aligned}
\hat{V}_{-1}^- &= \sum_{m=0}^{\infty}\left(\frac{\Omega^{m,1}}{2}|e\rangle\langle g| \otimes |m\rangle\langle m+1| + H.c.\right) \\
&= \sum_{m=0}^{\infty}\left(i\frac{|\Omega^{m,1}|}{2}|e\rangle\langle g| \otimes |m\rangle\langle m+1| e^{-i\phi} + H.c.\right)
\end{aligned} \tag{35}$$

$$\begin{aligned}
\hat{V}_1^+ &= \sum_{m=0}^{\infty}\left(\frac{\Omega^{m,1}}{2}|e\rangle\langle g| \otimes |m+1\rangle\langle m| + H.c.\right) \\
&= \sum_{m=0}^{\infty}\left(i\frac{|\Omega^{m,1}|}{2}|e\rangle\langle g| \otimes |m+1\rangle\langle m| e^{-i\phi} + H.c.\right)
\end{aligned} \tag{36}$$

Two superimposed laser fields at positive and negative detuning $\pm\nu$ from a common center frequency, respectively, produce a bichromatic light field. To arrive at a laser-ion interaction Hamiltonian describing this case, one can consider an ion simultaneously excited on the blue and red sideband:

$$\begin{aligned}\hat{V}_{bi} &= \hat{V}_{-1}^{-}(\phi_r) + \hat{V}_{1}^{+}(\phi_b) = \sum_{m=0}^{\infty} i\frac{|\Omega^{m,1}|}{2}\left((\sigma_+\sigma_{m,-}e^{-i\phi_r} + \sigma_+\sigma_{m,+}e^{-i\phi_b}) - H.c.\right) \\ &= \sum_{m=0}^{\infty} -\frac{|\Omega^{m,1}|}{2}\left((\frac{\sigma_x - i\sigma_y}{2}\sigma_{m,-}e^{-i(\phi_+ + \phi_-)} + \frac{\sigma_x - i\sigma_y}{2}\sigma_{m,+}e^{-i(\phi_+ - \phi_-)}) + H.c.\right) \\ &= \sum_{m=0}^{\infty} -\frac{|\Omega^{m,1}|}{2}\left(\sigma_x\sigma_{m,-}e^{-i\phi_-}\cos\phi_+ - \sigma_y\sigma_{m,-}e^{-i\phi_-}\sin\phi_+ + H.c.\right) \\ &= \sum_{m=0}^{\infty} -\frac{|\Omega^{m,1}|}{2}\left(\sigma_x\cos\phi_+ - \sigma_y\sin\phi_+\right)\left(\sigma_{m,+}e^{i\phi_-} + \sigma_{m,-}e^{-i\phi_-}\right) \end{aligned} \tag{37}$$

Where $\phi_+ = \frac{\phi_r+\phi_b}{2} + \frac{\pi}{2}$, $\phi_- = \frac{\phi_r-\phi_b}{2}$, $\sigma_{m,-} = |m\rangle\langle m+1|$ and $\sigma_{m,+} = |m+1\rangle\langle m|$

If the respective detuning of the bichromatic components is increased by an amount Δ to $\delta = \pm(\nu+\Delta)$, the light phases ϕ_L of the blue and red motional sidebands in (37) become time-dependent resulting in $\phi_r = \phi_r(0) - \Delta t$ and $\phi_b = \phi_b(0) + \Delta t$, respectively. In the bichromatic Hamiltonian given in (37) the time-dependence is only relevant in the difference phase $(\phi_r(0) - \phi_b(0))/2 - \Delta t$. Consequently, the M-S interaction is described by:

$$\hat{V}_{MS} = \sum_{m=0}^{\infty}\frac{|\Omega^{m,1}|}{2}\left(\sigma_{i,x} + \sigma_{j,x}\right)\left(\sigma_{m,+}e^{-i\Delta t} + \sigma_{m,-}e^{i\Delta t}\right) \tag{38}$$

Where it was assumed that $\phi_r(0) = \phi_b(0) = \pi/2$. Notice that $\hat{a} = \sum_{m=0}^{\infty}\sqrt{m+1}\,|m\rangle\langle m+1|$, $\hat{a}^\dagger = \sum_{m=0}^{\infty}\sqrt{m+1}\,|m+1\rangle\langle m|$ and $|\Omega^{m,1}| = |\lambda|\eta\sqrt{m+1}$. Then we can come back to the original $\hat{V}_{MS}$ as follows:

$$\hat{V}_{MS} = \frac{|\lambda|\eta}{2}(\sigma_{i,x} + \sigma_{j,x})(a^\dagger e^{-i\Delta t} + ae^{i\Delta t}) \tag{39}$$

(Notice: There is a more easy method to get above eqution directly from (9):
We expand the exponential term in (9) and only reserve the first order of η terms. Then we choose detuning $\delta = \nu + \Delta$ and $\phi = \phi_b$ for first blue sideband:

$$\hat{V}_{1}^{+}(\phi_b) = i\frac{|\lambda|\eta}{2}\left(\sigma_+ a^\dagger e^{-i(\Delta t+\phi_b)} - \sigma_- a e^{i(\Delta t+\phi_b)}\right)$$

and detuning $\delta = -(\nu + \Delta)$ and $\phi = \phi_r$ for first red sideband

$$\hat{V}_{-1}^{-}(\phi_r) = i\frac{|\lambda|\eta}{2}\left(\sigma_+ a e^{i(\Delta t-\phi_r)} - \sigma_- a^\dagger e^{-i(\Delta t-\phi_r)}\right)$$

Then the bichromatic field is:

$$\hat{V}_{bi} = i\frac{|\lambda|\eta}{2}\left(\sigma_+ a e^{i(\Delta t-\phi_r)} + \sigma_+ a^\dagger e^{-i(\Delta t+\phi_b)} - H.c.\right)$$

Then we set $\phi_b = \phi_r = \frac{\pi}{2}$, the $\hat{V}_{bi}$ becomes the same as (39).)

Then according to Magnus expansion[8] (`https://en.wikipedia.org/wiki/Magnus_expansion`) the evolution operator is as follows:

$$\begin{aligned}\hat{U}_{MS}(t) &= \exp\left(-i\int_0^t \hat{V}_{MS}(t_1)dt_1 - \frac{1}{2}\int_0^t dt_1\int_0^{t_1} dt_2\left[\hat{V}_{MS}(t_1),\hat{V}_{MS}(t_2)\right]\right)\\ &= \exp\left(-i\frac{(|\lambda|\eta)^2}{4}(\frac{t}{\Delta}-\frac{\sin(\Delta t)}{\Delta^2})\hat{S}_x^2\right)\exp\left(\frac{|\lambda|\eta}{2}\hat{S}_x\left(\frac{i}{\Delta}(e^{-i\Delta t}-1)a^\dagger + H.c.\right)\right)\\ &= e^{-i\Phi(t)\hat{S}_x^2}\left(1-\frac{\hat{S}_x^2}{4}+\frac{\hat{S}_x^2}{4}\cos\hat{\alpha}(t)+i\frac{\hat{S}_x}{2}\sin\hat{\alpha}(t)\right)\end{aligned} \tag{40}$$

Where $\Phi(t) = \frac{(|\lambda|\eta)^2}{4}\frac{t}{\Delta}(1-\frac{\sin(\Delta t)}{\Delta t})$ $\hat{S}_x = \sigma_{i,x}+\sigma_{j,x}$ and $\hat{\alpha}(t) = \frac{|\lambda|\eta}{\Delta}\left((e^{-i\Delta t}-1)a^\dagger - H.c.\right)$

If we set $\Delta t = 2n\pi$, then we will get:

$$\begin{aligned}\hat{U}_{MS}(2n\pi) &= e^{-i\Phi(2n\pi)\hat{S}_x^2} = e^{-in\pi(\frac{|\lambda|\eta}{\Delta})^2(1+\sigma_{i,x}\sigma_{j,x})}\\ &= e^{-in\pi(\frac{|\lambda|\eta}{\Delta})^2}\left(\cos\left(n\pi(\frac{|\lambda|\eta}{\Delta})^2\right) - i\sigma_{i,x}\sigma_{j,x}\sin\left(n\pi(\frac{|\lambda|\eta}{\Delta})^2\right)\right)\end{aligned} \tag{41}$$

Then we let $n=1$, $\Delta = 2|\lambda|\eta$ and get the transformation as follows:

$$\begin{aligned}\hat{U}_{MS} &= \frac{\sqrt{2}}{2}e^{-i\frac{\pi}{4}}(1-i\sigma_{i,x}\sigma_{j,x})\\ |g_i,g_j\rangle &\xrightarrow{\hat{U}_{MS}} |g_i,g_j\rangle - i\,|e_i,e_j\rangle\\ |g_i,e_j\rangle &\xrightarrow{\hat{U}_{MS}} |g_i,e_j\rangle - i\,|e_i,g_j\rangle\\ |e_i,g_j\rangle &\xrightarrow{\hat{U}_{MS}} |e_i,g_j\rangle - i\,|g_i,e_j\rangle\\ |e_i,e_j\rangle &\xrightarrow{\hat{U}_{MS}} |e_i,e_j\rangle - i\,|g_i,g_j\rangle\end{aligned} \tag{42}$$

IV. LASER COOLING TECHNIQUE

A. Doppler cooling[1]

We present a simple picture of doppler cooling of the ions. In this simple picture, micromotion is neglected and trapping potential is approximated by the time-independent pseudopotential $V(z) = \frac{1}{2}m\omega_z^2 z^2$. If the motion of the trapped ion is taken to be classical, its velocity obeys $v(t) =$

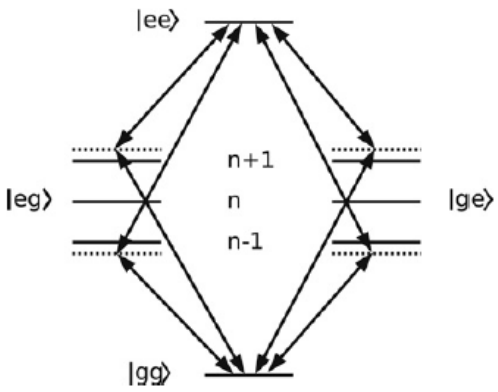

FIG. 2. MS gate process

$v_0 \cos(\omega_z t)$ If the radiative decay time $\frac{1}{\Gamma}$ is much shorter than one oscillation period $\omega_z \ll \Gamma$. One cycle of absorption and spontaneous emission occur in a time span where the ion does not appreciably change its velocity.

In this case the averaged radiation pressure can be modeled as a continuous force that depend on the ion's velocity. If the cooling laser is a single traveling wave along the ion's direction of motion, every absorption will give the ion a monmentum kick $\Delta\mathbf{p} = \hbar\mathbf{k}$ in the wave-vector direction of the photon, following by the spontaneous emission which will give the ion a random kick (average force is zero). So after many absorption-emission cycles, the ion will be slowed down.

The rate of absorption-emission cycle is given by the decay rate Γ times the probability of being in the excited state $\rho_{ee} = \langle e|\,\hat{\rho}\,|e\rangle$. Therefore the average force is $\left(\frac{d\mathbf{p}}{dt}\right)_a = \hbar\mathbf{k}\Gamma\rho_{ee}$ and $\Gamma\rho_{ee} = \Gamma\frac{|\lambda|^2/4}{\delta_e^2+|\lambda|^2/2+\Gamma^2/4} = \frac{\Gamma s/2}{1+s+(2\delta_e/\Gamma)^2}$[9] where $s = 2|\lambda|^2/\Gamma^2$, $\delta_e = \delta - \mathbf{k}\cdot\mathbf{v}$ is the doppler shift of the detuning.

$$\begin{aligned}\Gamma\rho_{ee} &= \frac{\Gamma s/2}{1+s+(2\delta/\Gamma)^2(1-\mathbf{k}\cdot\mathbf{v}/\delta)^2} \\ &= \frac{\Gamma s/2}{1+s+(2\delta/\Gamma)^2}\left(1+\frac{8\delta/\Gamma^2}{1+s+4\delta/\Gamma^2}\mathbf{k}\cdot\mathbf{v}\right)\end{aligned} \tag{43}$$

So the equation of motion of ions is:

$$\left(\frac{dp_z}{dt}\right)_a = -F_0(1-\kappa v_z) \tag{44}$$

minus sign before F_0 means the positive direction is atom's velocity direction. Where $F_0 = \frac{\hbar k\Gamma s/2}{1+s+(2\delta/\Gamma)^2}$ and $\kappa = \frac{8k\delta/\Gamma^2}{1+s+(2\delta/\Gamma)^2}(<0)$

Doppler cooling limit:

Consider a laser beam is along the z-axis, the atom's motion is also along the z direction.

$$\frac{d}{dt}(\frac{1}{2}mv_z^2) = v_z\frac{dp_z}{dt} = -v_zF_0(1-\kappa v_z) \tag{45}$$

The cooling rate is:

$$\begin{aligned}\dot{E}_c &= \langle\frac{d}{dt}(\frac{1}{2}mv_z^2)\rangle = -F_0\langle v_z\rangle + F_0\kappa\langle v_z^2\rangle \\ &= F_0\kappa\langle v_z^2\rangle (< 0)\end{aligned} \tag{46}$$

We deduce the heating rate below[9]:

A force from the single laser beam is $\mathbf{F} = \mathbf{F}_{abs} + \delta\mathbf{F}_{abs} + \mathbf{F}_{spont} + \delta\mathbf{F}_{spont}$. $\mathbf{F}_{abs}$ corresponds to cooling force and $\mathbf{F}_{spont} + \delta\mathbf{F}_{abs} + \delta\mathbf{F}_{spont}$ corresponds to heating force. $\mathbf{F}_{spont}$ is averaged to zero. What we never consider is the fluctuation of $\mathbf{F}_{abs}$ and $\mathbf{F}_{spont}$ that will cause heating rate.

The spontaneous emission that always accompanies $\mathbf{F}_{abs}$ causes the atom to recoil in random directions. These recoil kicks lead to a random walk of the velocity. A random walk of N steps gives a mean square displacement equals N times the square of the step length. During a time t, an atom scatters a mean number of photons $N = R_{scatt}t = \Gamma\rho_{ee}t$, spontanesous emission causes the mean square momentum to increase as $\overline{p^2} = \Gamma\rho_{ee}t(\hbar k)^2$, along the z-axis, we should add a scaling factor $\overline{p_z^2} = \xi\Gamma\rho_{ee}t(\hbar k)^2$.

The fluctuation $\overline{\delta\mathbf{F}_{abs}}$ arises because the atom does not always absorb the same number.Each absorption is followed by spontaneous emission and the mean number of such events in time t is given by $N = \Gamma\rho_{ee}t$. Assuming that the scattering obeys Poissonian statistics, the fluctuation about the mean have a standard deviation of $\sqrt{N}$ and cause a random walk of the momentum along the laser beam.

This one-dimensional random walk caused by the fluctuation $\overline{\delta\mathbf{F}_{abs}}$ leads to an increase in the momentum spread to $\overline{p^2}$ without any scaling factor because the random walk is only in one dimension. So the total heating rate is $\left(\frac{\overline{p^2}}{2m}\right)' = \frac{\Gamma\rho_{ee}(\hbar k)^2(1+\xi)}{2m}$. Let the cooling rate equals heating rate:

$$\frac{\Gamma\rho_{ee}(\hbar k)^2(1+\xi)}{2m} = F_0|\kappa|\langle v_z^2\rangle$$

$$\begin{aligned}k_BT = m\langle v_z^2\rangle &= \frac{\hbar\Gamma}{8}(1+\xi)((1+s)\frac{\Gamma}{2|\delta|} + \frac{2|\delta|}{\Gamma}) \\ &\geq \frac{\hbar\Gamma}{4}(1+\xi)\sqrt{1+s}\end{aligned} \tag{47}$$

When $|\delta| = \frac{\Gamma}{2}\sqrt{1+s}$, we can reach the doppler cooling limit temperature:

$$T_D = \frac{\hbar\Gamma}{4k_B}(1+\xi)\sqrt{1+s} \tag{48}$$

B. resolved sideband cooling[1][10]

1. *direct sideband cooling*

The sidebands on the optical spectrum correspond to transitions between the vibrational levels of the trap. Specifcally, if a two-level atom has a ground state $|g\rangle$ and excited state $|e\rangle$, with vibrational states labelled by n, then exciting on a sideband corresponds to the transition $|g,n\rangle \leftrightarrow |e,n'\rangle$. Hence, if a laser is tuned to the first lower sideband(21), it will excite the $|g,n\rangle \leftrightarrow |e,n-1\rangle$ transition. When the atom spontaneously decays, it has the highest probability of decaying on the carrier (i.e. with no change in n), and so on average one quantum ($\hbar\omega_{sec}$) of vibrational energy is taken from the ion's motion in each cycle. The cooling process is illustrated in Figure 3 To resolve

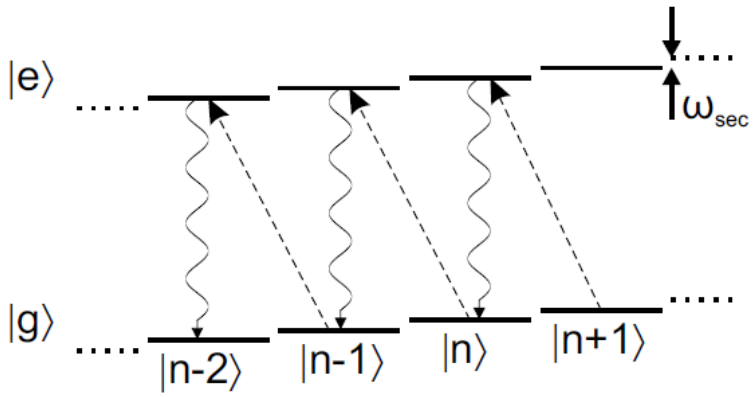

FIG. 3. resolved side band cooling with first red detuning laser

the sideband, the excited state should be narrow in linewidth. So the spontaneous decay rate Γ should be far smaller than ω_{sec}. For this reason, sideband cooling cannot use the electric dipole transitions typically used for Doppler cooling. Usually, an electric quatrupole transition is used, with a long life time in the order of 1 s, i.e. the linewidth in the order of 1 Hz. However, because of the very narrow linewidth, the spontaneous rate is very low, we should add a quench light to increase the cooling efficiency. Figure 4 show the level scheme of $^{40}Ca^{+}$, the sideband cooling light couples the S and D levels, and the quench light couples the D and P levels.

2. *Raman sideband cooling*

Raman side band cooling is very similar to direct sideband cooling. In the latter case, one red detuning light couples quatrupolely between the ground state and a long lifetime excited

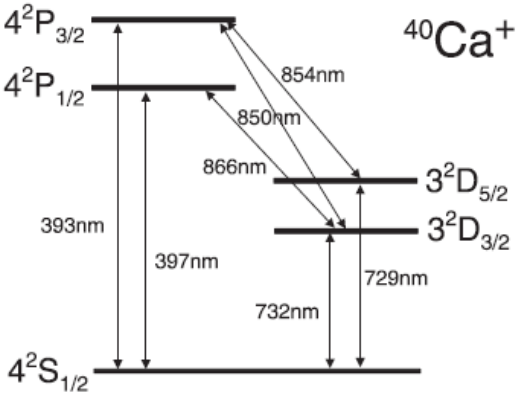

FIG. 4. level scheme of calcium40+

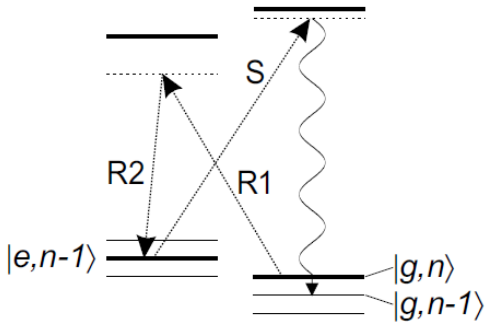

FIG. 5. Raman cooling scheme

state. However, in the Raman sideband cooling scheme, see figure 5, two Raman beams with a frequency difference $\omega_0 - \omega_{sec}$ illuminate ions at the same time, though both Raman beams will be actually derived from the same laser via an AOM. Then a quenching light also illuminate the ions to increase the cooling efficiency. As a specific example, let's see the Raman sideband cooling in $^{171}Yb^+$. Two Raman beams with a frequency difference around 12.6 GHz (the energy difference between $^2S_{1/2}\,|F=0\rangle$ and $^2S_{1/2}\,|F=1,m_F=0\rangle$ states). Also, a quenching light couples $^2S_{1/2}\,|F=1,m_F=0\rangle$ with $^2P_{1/2}\,|F=1,m_F=0\rangle$

C. heating rate of motional state

V. DECOHERENCE IN ION TRAP

VI. IMAGE SYSTEM

A. Introduction

Ions are illuminated by detection laser and will be excited to a very short-lifetime level (∼ns), so they will spontanesouly decay and emit photons. Then photons will be collected by the image system. This image process is a typical florescence imaging[11]. All fluorescence imaging systems require the following key elements

- Excitation source
- Light delivery optics
- Light collection optics
- Filtration of the emitted light
- Detection, amplification and digitization

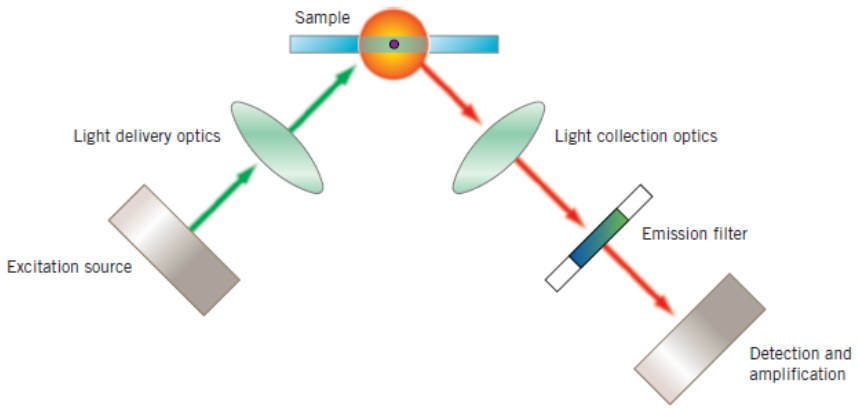

FIG. 6. floresence imaging system

In our $^{171}Yb^{+}$ ion trap, the excitation source is a 370nm laser. The light delivery system is very complicated and will delay to introduce it. The light collection system is of most importance, because the spontaneous emission is random in all direction and only a fraction of light will be

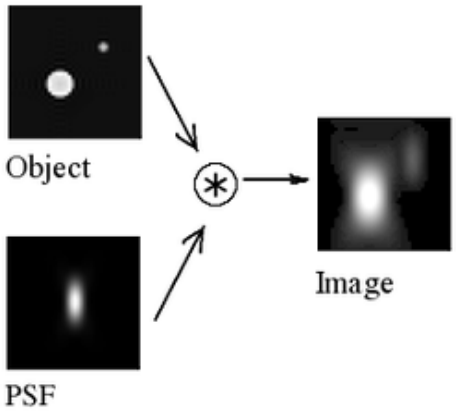

FIG. 7. object field convolves with PSF and get the image field

collected through the optics collection system. For this reason, the collection system must as efficient as possible. Also the resolution and magnification of the system should be considered. It will be introduced later. The filtration of the emitted light is a narrow bandwidth light filter to prevent some stray light disturbance. The detection system is a EMCCD and a PMT.

B. Modeling the image process[12]

In non-coherent imaging systems such as fluorescent microscopes, telescopes or optical microscopes, the image formation process is linear in power and described by linear system theory. This means

$$Image(Object1 + Object2) = Image(Object1) + Image(Object2)$$

In a more mathematical form

$$\hat{I}(O_A(x,y) + O_B(x,y)) = \hat{I}(O_A(x,y)) + \hat{I}(O_B(x,y)) \tag{49}$$

where $\hat{I}$ can be seen as an image operator, $O(x,y)$ is the object field in the 2D object plane. The image operator is $P(x,y)*$, it operate on the object field means the function $P(x,y)$ convolve with the function $O(x,y)$. The function $P(x,y)$ is the so called point spread function (PSF). It is determined by all of the components of the image system. In principle, if we can calculate the PSF, we can calculate the image field in the image plane as seen from figure7. However, calculating the PSF of a specific component by hand is a very hard task, we can use some software like "Huygens" to calculate it.

$$I(x,y) = \iint O(\alpha,\beta)P(x-\alpha, y-\beta)d\alpha d\beta \tag{50}$$

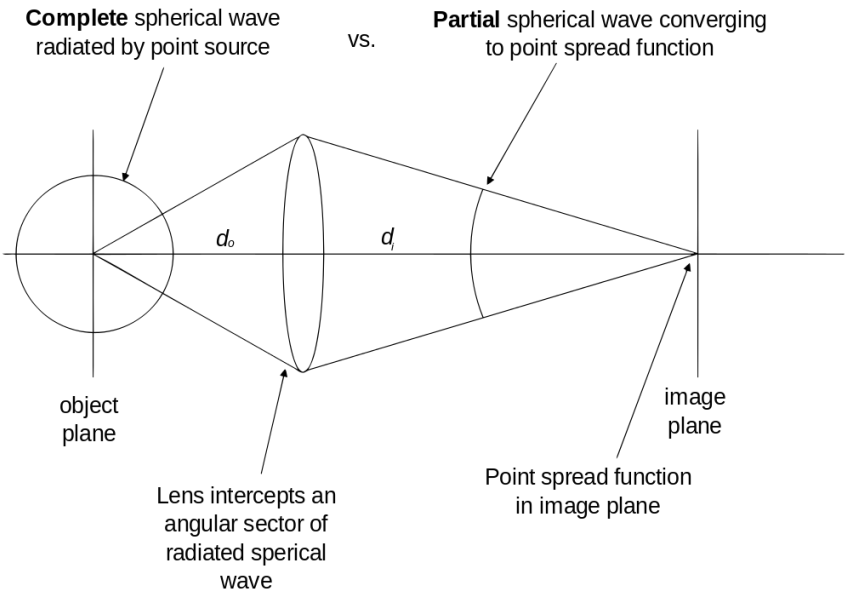

FIG. 8. Truncation of Spherical Wave by Lens

if the object field is a point source,then

$$I(x,y) = \iint \delta(\alpha - x_0, \beta - y_0) P(x-\alpha, y-\beta) d\alpha d\beta = P(x_0, y_0) \tag{51}$$

i.e. the image of a point source is the PSF of the image system. Let us consider a simple case, see figure8, an ideal lens[13] intercepts a portion of a spherical wave from a point source and refocuses it onto a blurred point in the image plane. For a single lens, an on-axis point source in the object plane produces an Airy disc PSF in the image plane, therefore, the converging (partial) spherical wave shown in the figure8 produces an Airy disc in the image plane. Airy disc is the central disc of the Airy function, figure9, and its half angular size is $\theta = 1.22\lambda/D$, where λ is the wavelength and D is the clear apeture of the lens.

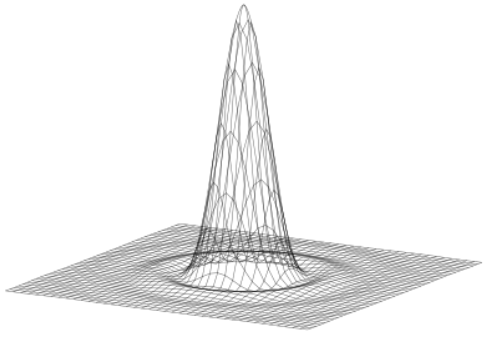

FIG. 9. Airy function

C. specific system design

The light collection systems in different ion trap groups are largely identical[8]. There are usually two stages of imaging. One is from ion through a customed objective to an iris, the other is from the iris through a lens assembly to the CCD sensor. This design using the iris can spatially filter out any background scattered light outside the desired field of view of the objective.

In this section, we will introduce a specific light collection system design[8]. See figure10. Their

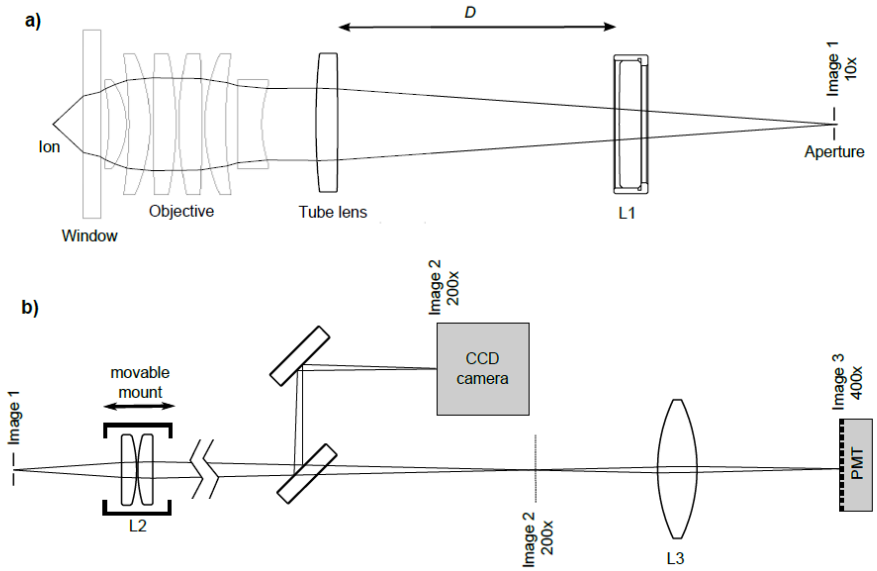

FIG. 10. imaging system design from Monroe group for detection

objective11 is customed from Photo Gear and have a 0.38 N.A.. Higher N.A. means larger solid angle and can enhance florescence collection effiency and resolution. From Abbe resolution formula $R = 0.61\lambda/N.A.$, we can estimate the resolution of the objective and it is about 600nm. It's more than sufficient for the ion string resolution because the space between ions is around $5\mu m$. The light from ion trough the objective should be collimated and focused using a 200mm focal length best form lens from Thorlabs[14] with roughly $\times 10$ magnification.

The collimated light can be regarded as from infinity and we use Fraunhofer diffraction to estimate the spot size after the best form lens. $1.22\lambda f/D$ and is around $6\mu m$. It seems to be consistent with the magnification. Then an iris set at $200\mu m \times 1000\mu m$ apeture, this means the field of view is $20\mu m \times 100\mu m$, is placed at the focal plane to spatially filter out any stray light outside the field of view.

After the iris, the light goes into a Ramsden like eyepiece and refocuses into the CCD sensor. The eyepiece is mounted onto a movable stage and can be adjusted from the iris to change the second

stage magnification.

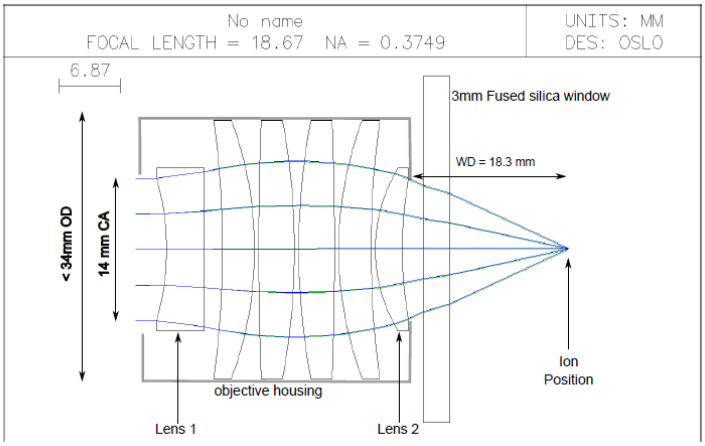

FIG. 11. objective from Photo Gear

Our CCD is Andor iXon blue DU-897-DCS-BBB, 512×512 pixels of $16 \times 16 \mu m$ size, the same as reference[7]. According to this thesis12, their image system has a magnification of 24.6, ion space is around $4.87 \mu m$ so the pixels population is about 7.49 px. The FWHM of the intensity of the sensor is around 2.13 px so the ion spot size is about $1.4 \mu m$ basically matching the diffraction-limited resolution (N.A.=0.289). Generally, the ion can be seen as a point light source after doppler cooling[15].

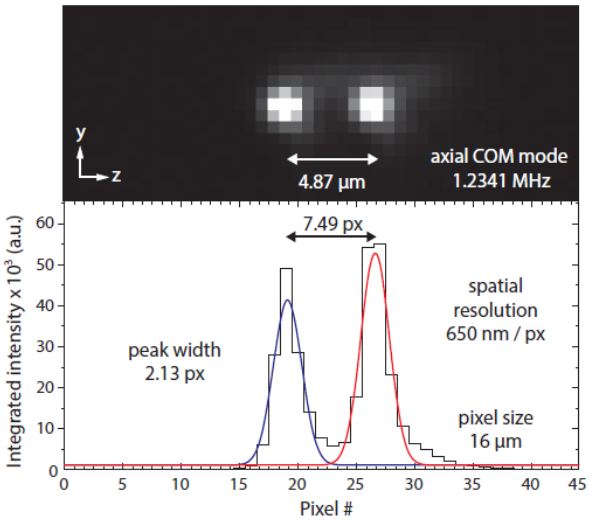

FIG. 12. camera detection

VII. ELECTRONIC SYSTEM IN ION TRAP EXPERIMENT

There are so many electronic devices in ion trap experiment. They can be divided into several parts such as electronic system for trap voltage supply, electronic system for AOM/EOM driving, electronic system for laser stabilization, etc. We will introduce all of them in the following sections.

A. RF/DC voltage supply system

For room temperature ion trap, the rf voltage is supplied by usual helical resonator[16], the rf frequency is usually tens of megahertz and the voltage is usually hundreds of volt. For cryogenic ion trap, the rf resonator should be specially designed such that can be set inside the thermostat and isolated from the outside[17].

As for the DC supply, there are roughly two types. One is lower voltage for surface trap and the other is high voltage for normal trap design (four-rod trap, blade trap, etc.). For the latter, commercial high voltage source is suited for supplying hundreds-of-volt voltage. And for the surface trap, the voltage is tens of volt and there are many choices. Usually, on-board DAC with operational amplifier is a good choice. Sometimes a commercial storage battery also can be used as DC supply.

B. electronic system for AOM/EOM driving

Both AOM and EOM can be driven by a radio-frequency signal source with an amplifier. In experiment, we may add some modulation to aom driving signal, so the voltage-controlled oscillator (VCO) is used to drive it. The frequency of VCO is controlled by a voltage input, i.e. the input voltage determined the instantaneous oscillation frequency. Consequently, modulating signals applied to control input may cause frequency modulation (FM) or phase modulation (PM). This is important to experiment, because almost all the modulation adding to laser and then changing the Hamiltonian of ion-laser interaction is caused by adding modulation to AOM. Also in many laser frequency stabilization scheme such as gas-reference locking technique[18], modulation to AOM is necessary. The input of the VCO may be a DC voltage (generating carrier frequency) plus a small voltage modulating signal, so a DC-RF adder (bias tee) is necessary[19].

For EOM driving, a AD9910 dds is enough for low frequency driving. For high frequency driving such as 2.1GHz, 3.1GHz, 3.6GHz, 14.75GHz in $^{171}Yb^{+}$ experiment, a brick-like signal source (maybe from Labbrick) is a good choice.

C. electronic system for laser stabilization

For laser frequency stabilization, the electronic devices can roughly be divided into two parts, one is demodulation part, the other is servo control part, no matter what the scheme of the frequency stabilization is. For $^{171}Yb^{+}$ ion experiment, the 370nm laser is very important, we adopt modified PDH scheme[20] or hollow cathode lamp[18] to stabilize the laser frequency. For the first scheme, the demodulation system can be set up by the rf devices from mini-circuits including mixers, low pass filters and phase shifters. The servo controller can be homemade PID or module from TOPTICA such as FALC 110. There are many frequency stabilization modules from TOPTICA, the mFALC 110 is a mixer plus a high speed PID; the FALC 110 is a high speed PID; the PDD110/F is a signal source plus a demodulation system. For the hollow cathode lamp scheme, a digital lock-in amplifier can be used as demodulation system. We copy a lock-in amplifier from NIST group, also we can use the built-in lock-in amplifier and PID of the TOPTICA DLC pro as the demodulation system and servo control system. We also by the model lb2001(servo controller) and lb2005(demodulator) from Sacher lasertechnik as the frequency stabilization system.
For laser intensity stabilization, servo controller is also needed. It feeds back to VVA(voltage variable attenuator) between the signal source and AOM.

---

[1] D. Leibfried, R. Blatt, C. Monroe, and D. Wineland. Quantum dynamics of single trapped ions. *Rev. Mod. Phys.*, 75:281–324, Mar 2003.

[2] Sasura Marek and Buzek Vladimir. Cold trapped ions as quantum information processors. *Journal of Modern Optics*, 49(10):1593–1647, 2002.

[3] Hubert Tony. Stimulated raman transitions between hyperfine ground states of magnetically trapped rubidium-87 atoms, 2015.

[4] J. I. Cirac and P. Zoller. Quantum computations with cold trapped ions. *Phys. Rev. Lett.*, 74:4091–4094, May 1995.

[5] Anders Sørensen and Klaus Mølmer. Quantum computation with ions in thermal motion. *Phys. Rev. Lett.*, 82:1971–1974, Mar 1999.

[6] Anders Sørensen and Klaus Mølmer. Entanglement and quantum computation with ions in thermal motion. *Phys. Rev. A*, 62:022311, Jul 2000.

[7] Cornelius Hempel. *Digital quantum simulation, Schrödinger cat state spectroscopy and setting up a linear ion trap.* PhD thesis, University of Innsbruck, 2014.

[8] Shantanu Debnath. A programmable five qubit quantum computer using trapped atomic ions, 2016.

[9] Christopher J. Foot. *Atomic physics*. Oxford master series in physics 7. Atomic, Optical, and laser physics. Oxford University Press, 1 edition, 2005.

[10] Peter James Blythe. *Optical frequency measurement and ground state cooling of single trapped Yb+ ions*. PhD thesis, University of London, 2005.

[11] Vasilis Ntziachristos. Fluorescence molecular imaging. *Annual Review of Biomedical Engineering*, 8(1):1–33, 2006. PMID: 16834550.

[12] K. Fliegel. Modeling and measurement of image sensor characteristics. *Radioengineering*, 13(4):0–, Dec. 2004.

[13] Here ideal means the lens is a diffraction-limited system.

[14] LBF254-200-A.

[15] J. D. Wong-Campos, K. G. Johnson, B. Neyenhuis, J. Mizrahi, and C. Monroe. High-resolution adaptive imaging of a single atom. *nature photonics*, 10, Jul 2016.

[16] J. D. Siverns, L. R. Simkins, S. Weidt, and W. K. Hensinger. On the application of radio frequency voltages to ion traps via helical resonators. *Applied Physics B Lasers and Optics*, 107(4):921–934, 2012.

[17] M. F. Brandl, P. Schindler, T. Monz, and R. Blatt. Cryogenic resonator design for trapped ion experiments in paul traps. *Applied Physics B*, 122(6):157, 2016.

[18] M. W. Lee, M. C. Jarratt, C Marciniak, and M. J. Biercuk. Frequency stabilization of a 369 nm diode laser by nonlinear spectroscopy of ytterbium ions in a discharge. *Optics Express*, 22(6):7210–21, 2014.

[19] Matthew Aldous, Jonathan Woods, Andrei Dragomir, Ritayan Roy, and Matt Himsworth. Carrier frequency modulation of an acousto-optic modulator for laser stabilization. *Opt. Express*, 25(11):12830–12838, May 2017.

[20] Gatan Hagel, Marie Houssin, Martina Knoop, Caroline Champenois, Michel Vedel, and Fernande Vedel. Long-term stabilization of the length of an optical reference cavity. *Review of Scientific Instruments*, 76(12):233, 2005.